

In-Situ Passivation Perovskite Targeting Efficient Light-Emitting Diodes via Spontaneously Formed Silica Network

Yuqiang Liu,^{1,2} Lei Cai,¹ Yafeng Xu,¹ Junnan Li,¹ Yuanshuai Qin,¹ Tao Song,¹ Lu Wang,¹
Youyong Li,¹ Luis K. Ono,² Yabing Qi,^{2*} Baoquan Sun^{1*}

¹ Jiangsu Key Laboratory for Carbon-Based Functional Materials and Devices, Institute of Functional Nano & Soft Materials, Joint International Research Laboratory of Carbon-Based Functional Materials and Devices, Soochow University, Suzhou 215123, China

² Energy Materials and Surface Sciences Unit (EMSSU), Okinawa Institute of Science and Technology Graduate University (OIST), Okinawa 904-0495, Japan

*Corresponding authors: Yabing.Qi@OIST.jp (Y. B. Q.); bqsun@suda.edu.cn (B. S.).

Abstract

Perovskite materials are attractive candidates as emitting layers in light-emitting diodes due to their excellent optical and electrical properties. Effective charge radiative recombination is a key to target high-efficiency perovskite light-emitting diodes (PeLEDs). State-of-the-art effective passivation chemicals in PeLEDs mostly belong to organic chelating molecules, associated with like molecular detachment in the device operation, which simultaneously degrades the performance especially the operational stability of the devices. Here, a silane material tetraethoxysilane (TEOS), which can be crosslinkable to avoid any likely detachment from perovskite film, is incorporated into the perovskite film to enhance film radiative recombination and stability. An oxo-bridged silica network anchored with perovskite is formed after the TEOS *in-situ* crosslinking process. It is found that the lone pair electrons in TEOS network can coordinate with the undercoordinated Pb^{2+} of perovskite. Consequently, defect states in perovskite film are dramatically diminished, which enhances radiative recombination. The photoluminescence intensity of resultant perovskite-TEOS film is enhanced by 40% over that of the pristine one. The average photoluminescence lifetime of perovskite-TEOS film reaches 58 ns, enhanced by 65% over that of the pristine perovskite film of 35 ns. As a result, a green PeLED achieved an external quantum efficiency of 16.6% with improved working stability. This work presents a facile strategy targeting efficient and stable perovskite devices *via* utilizing detachment-free self-crosslinked ligands.

Keywords: Perovskite; Light-emitting diodes; Crosslinking; Non-radiative recombination

Introduction

Perovskite materials attract wide attention in the field of light-emitting diode (LED) owing to their excellent optoelectrical properties such as high photoluminescence quantum efficiency (PLQE), widely tunable emission range, and superior color purity.[1-4] Since a room-temperature perovskite LED (PeLED) with an external quantum efficiency (EQE) below 1% was reported,[5] several strategies including doping,[6-8] confinement,[9-11] colloidal nanocrystal,[12-16] and passivation[17-19] have been witnessed to enhance the device performance. Up to now, impressive efficiencies have been achieved in near-infrared, red, green and blue colors,[20-23] and the champion EQE has reached 21.6% in near-infrared PeLEDs.[24] Radiative recombination of injected charges followed by emission of photons is the critical process of efficient PeLEDs. However, due to the small exciton binding energy in bulk three-dimensional halide perovskites, electron-hole pairs display a large possibility of dissociation instead of radiative recombination. Two-dimensional (2D) perovskite materials with a quantum-well structure present an alternative method to dramatically enhance the exciton binding energy, due to their dielectric or quantum confinement.[25, 26] Phenylethylammonium (PEA) bromide was incorporated into a precursor solution as chelating agent to confine the perovskite growth, where there is strong interaction between free pair electrons of nitrogen in PEA and Pb^{2+} in perovskite, which strengthened the ratio of radiative recombination *via* the funneling mechanism. A *quasi* 2D perovskite in the resultant film delivered an infrared emitting device with an EQE of 8.8%.[27] Similarly, naphthylmethylamine (NMA) bromide was utilized as chelating agent to confine perovskite growth, and an infrared emitting device with an EQE of 12.7% is achieved due to the increased radiative recombination in multiple quantum wells.[28] Unfortunately, the incorporation of these organic constituents (*i.e.* PEA, NMA) likely blocks the energy funneling process among *quasi*-2D perovskite materials due to their phase aggregation between organic ligand and perovskite.

To resolve this issue, an cyclic oligomers of ethylene oxide, consisting of the repeating unit being ethyleneoxy which can interact with organic ligand and cations in perovskite, is incorporated into perovskites film to suppress the phase aggregation as well as anchoring surface passivation agent simultaneously, and the resultant film offer a green-emitting device

with an EQE of 15.5%. [29] Meanwhile, poly(2-hydroxyethyl methacrylate), each monomer consisting of one ester and one hydroxy groups which can strong chelating with lead in perovskite, is incorporated to reduce the defect state, and an infrared emitting device with an EQE of 20.1% is achieved. [30] As aforementioned above, all the ligand chelating with lead in perovskite used for reducing defect state is organic small molecule, either detachment from lead or self-aggregation would occur, which would deteriorate the PeLED device performance in the operated process especially at high voltage. Passivation is an effective solution to eliminate defects and consequently reduce non-radiative recombination losses. [31] Lewis bases demonstrated a general passivation effect in perovskite solar cells. [32-36] The lone pair electron groups on Lewis bases, such as hydroxyl groups (-OH), carboxyl groups, and carbonyl groups, can coordinate with the undercoordinated Pb^{2+} in perovskite materials, which can passivate the defect states effectively. Meanwhile, crosslinking method is promising to improve the quality of perovskite nanocrystals. [37]

Herein, a Lewis base silica tetraethoxysilane (TEOS), consisting of four hydroxy groups, is incorporated into perovskite film to anchor with lead in order to suppress the defect states. Compared with previous passivation additives, [30, 38, 39] TEOS, which is not vaporized, not only has the passivation effect, but also self-crosslinks into a network during the formation process of perovskite film. The TEOS is polymerized into a network after the hydrolysis processes, which would avoid any likely detachment from perovskite. The PL intensity of resultant perovskite with TEOS (perovskite-TEOS) is enhanced by 40%, compared with that of the pristine one. In addition, the average PL lifetime of perovskite increased from 35 ns to 58 ns after incorporating TEOS. Finally, radiative recombination is enhanced, and an EQE of 16.6% is achieved in green PeLEDs with improved stability.

Experimental section

Materials and devices fabrication

For the 2D $PEA_2Cs_{n-1}Pb_nBr_{3n+1}$ perovskite film fabrication, the precursor solution was prepared by dissolving CsBr (0.2 mmol), $PbBr_2$ (0.2 mmol), PEABr (0.08 mmol), and crown (4.0 mg) in 1 mL DMSO solution with or without 5 μ L TEOS, followed by stirring for 4 h. Cleaned ITO

substrates were treated by oxygen plasma for 15 min. The nickel oxide (NiO_x) and poly(9-vinylcarbazole) (PVK) film were deposited onto the indium tin oxide (ITO) glass according to the previous report.[40] Afterwards, the perovskite precursor solution was spin-coated onto the NiO_x/PVK film at 1000 rpm for 5 s and 4000 rpm for 55 s, and then annealed at 100 °C for 5 min in a nitrogen glovebox. 2,2',2''-(1,3,5-benzenetriyl) tris-(1-phenyl-1Hbenzimidazole) (TPBi, 40 nm), lithium fluoride (LiF, 1 nm) and aluminum (Al, 100 nm) were evaporated onto the perovskite film sequentially in a thermal evaporation chamber with vacuum pressure of lower 2×10^{-6} mbar. The active area of device is 0.09 cm².

DFT computational method

The DFT calculations were implemented in the Vienna ab initio simulation package (VASP).[41, 42] The Perdew-Burke-Ernzerhof (PBE) functional [43, 44] was used to describe the electron-electron exchange correlation and the projector augmented wave (PAW) method [45] was chosen to describe the ion-electron interaction. We also considered the van der Waals interaction in the systems by using DFT-D3 correction.[46] The kinetic energy cutoff for the plane wave basis sets was defined as 500 eV. The structures are relaxed until the forces acting on all atoms are less than 0.02 eV Å⁻¹. The 2×2 supercell associated with 2×2×1 Monkhorst-Pack k-point grids are used.

Device characterization

The crosslinked network on 2D perovskite was investigated by FTIR spectrometer (Bruker Optics, VERTEX 70). The top surface morphology and cross-sectional images of complete PeLED devices were acquired by a field emission SEM (Zeiss Spira55). Energy dispersive X-ray detector (EDX) was investigated by SEM (JEOL, JSM-7900F). Surface morphology and root-mean-square (RMS) roughness were measured by atomic force microscopy (AFM, Veeco Multimode V). Crystal structure determination of 2D perovskite with and without TEOS were investigated by X-ray diffractometer (PANalytical B.V. Empyrean, Cu Kα source). Absorption was measured by a UV-Vis spectrophotometer (Specord S600). Steady-state PL spectra and time-resolved PL spectra were measured by a fluorescence spectrophotometer (HORIBA-FM-2015). XPS spectra were recorded from an X-ray photoelectron spectrometer (XPS-AXIS Ultra HAS, Kratos). Optoelectronic parameters were tested by a photoresearch spectrometer PR670 and a Keithley 2400 source-meter.

Results and discussion

The device structure is ITO/NiO_x/PVK/perovskite/TPBi/LiF/Al. The perovskite emitting layer (~60 nm) is 2D PEA₂Cs_{n-1}Pb_nBr_{3n+1} film with or without TEOS (Figure S1), where $\langle n \rangle$ is the layer number of the perovskite nanoplatelet. The alkoxy group of TEOS can be gradually hydrolyzed and converted into the silanol in the perovskite solution. Then, the hydrolyzed TEOS builds a crosslinked network,[47] as exhibited in Figure 1a. Figure 1b illustrates the formation procedure of a crosslinked TEOS-perovskite film. Associated with perovskite phase formation, hydrolyzed TEOS is polymerized into a network *in situ*. Additionally, due to the interaction between the Pb²⁺ on perovskite and the oxygen on TEOS network, TEOS is likely anchored with perovskite, and consequently, a composite of crosslinked TEOS and 2D perovskite film is built.

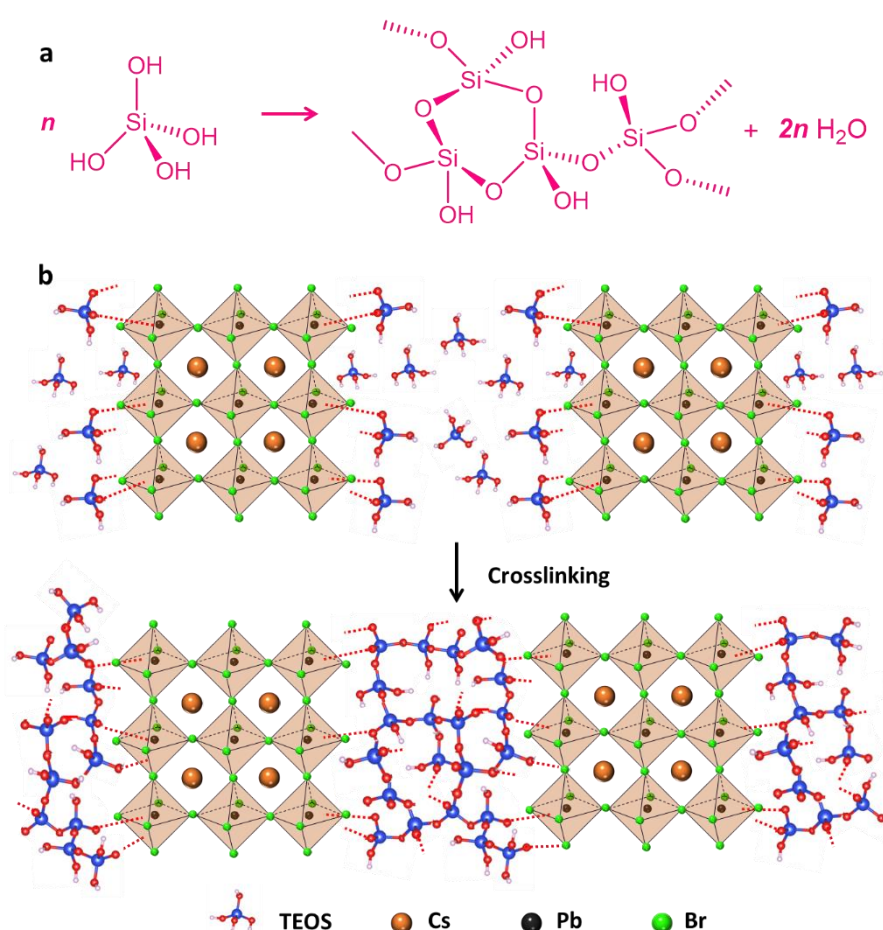


Figure 1. Formation schematic of (a) crosslinked TEOS network and (b) crosslinked TEOS-2D perovskite composite film.

Fourier transform infrared spectroscopy (FTIR) measurements confirm that there are numerous hydroxy groups in the composite film. As shown in Figure 2a, according to FTIR spectra of perovskite and TEOS, there are strong vibrational peaks located at 1115 cm^{-1} and 1090 cm^{-1} in the TEOS film, which are ascribed to the longitudinal optical and the transversal optical modes of the Si-O-Si stretching vibrations, respectively.[47] These vibrations verify the existence of oxo-bridged silica formation in the composite film. In addition, it can be inferred that there are Si-OH groups in the TEOS film according to vibration mode peak at 964 cm^{-1} . There are two strong peaks at 1082 cm^{-1} and 957 cm^{-1} in the perovskite-TEOS film, which are ascribed to Si-O-Si and Si-OH groups, respectively. The FTIR measurement reveals TEOS hydrolyzation occurring. It worth noting that the peaks for perovskite-TEOS film are shifted to lower wavenumbers, which is likely ascribed to interaction between undercoordinated Pb^{2+} on perovskite and oxygen on the TEOS network.[48, 49] The Lewis adduct decreases the stretching force and consequently produces a lower wavenumber shift of the vibrations. Generally, a crosslinked network would be formed once TEOS hydrolyzing, therefore, it would be deduced that Si-O-Si network is built between the grain boundary of perovskite. EDX mapping further determines the existence of TEOS in perovskite films, according to the spatial distribution of Cs, Pb, Br and Si elements in Figure S2.

Scanning electron microscopy (SEM) images of perovskite and perovskite-TEOS deposited onto NiO_x/PVK are shown in Figures 2b and c, no obvious difference is observed. Atomic force microscopy (AFM) measurements were also conducted to probe the surface morphology. As shown in Figure S3, both films display a similar root mean square roughness (RMS) value of $\sim 1.6\text{ nm}$. The above SEM and AFM measurements indicate that TEOS displays minimum influence on the film morphology leading to uniform and full covered 2D perovskite films. Furthermore, the smooth surfaces (*i.e.*, low RMS) is beneficial for attaining high device performance.[50, 51] Figure S4 corresponds to the absorption curves of 2D perovskite films with and without the TEOS, and the same absorption peaks are observed. This indicates the incorporation of TEOS does not change the bandgap ($\sim 2.35\text{ eV}$) of the perovskite. Meanwhile, X-ray diffraction patterns are measured to study the crystallinity of perovskite films, as shown in Figure S5. The diffraction peaks with 2θ values of 15.2° and 30.5° correspond to the (100) and (200) plane reflection, respectively.[29] According to the Scherrer equation, the perovskite

crystal sizes extracted from (200) peaks are ~ 8.0 nm and ~ 7.8 nm for with and without TEOS, respectively. These phenomena demonstrate that the incorporation of the TEOS has a negligible influence on the optical properties and the crystal structure of 2D perovskite films.

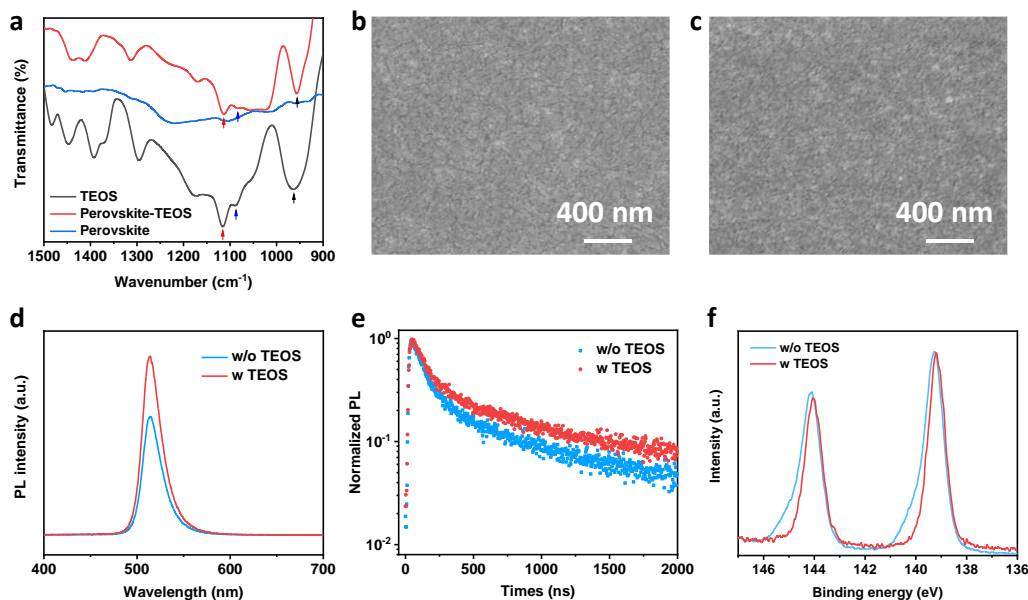


Figure 2. (a) FTIR spectra of perovskite, TEOS network and perovskite-TEOS. SEM image of (b) perovskite and (c) perovskite-TEOS films on NiO_x/PVK films. (d) Steady-state PL spectra, (e) Time-resolved PL spectra, and (f) XPS spectra for $\text{Pb } 4f_{7/2}$ and $\text{Pb } 4f_{5/2}$ of perovskite and perovskite-TEOS films.

TEOS incorporation can enhance the steady-state photoluminescence (PL) intensity as well as PL lifetime. As shown in Figure 2d, both PL peaks are located at 514 nm. The PL intensity of perovskite-TEOS is enhanced by 40%, compared with that of the pristine one. Meanwhile, the PL lifetime increases in perovskite-TEOS, as shown in Figure 2e. According to a triexponential fitting, the average PL lifetime of perovskite-TEOS film reaches 58 ns, enhanced by 65% over that of the pristine perovskite film (35 ns). The PL quantum yield (Figure S6) of perovskite films without and with TEOS are 43.5% and 56.5%, respectively. The undercoordinated Pb^{2+} ions on 2D perovskite serving as defect states form deep-level defect state centers, which enhance the probability of charge non-radiative recombination events.[52] The oxygen on the TEOS involving lone pair electrons can coordinate with these Pb^{2+} ions. This can passivate the electronic defect states, and non-radiative recombination channel is suppressed. X-ray

photoelectron spectroscopy (XPS) provides insight into the local binding environment of surface chemical states and the binding energy of the atoms. As shown in Figure 2f, the core levels of both peaks of Pb 4f_{7/2} and Pb 4f_{5/2} shift toward lower binding energies, which indicates that the lead chemical environment has changed in the presence of TEOS. The lone pair electrons on TEOS could donate electrons to undercoordinated Pb²⁺ ions, which coordinates Pb²⁺ ions, resulting shift to lower binding energies.[53]

The space charge limited current (SCLC) is measured to estimate the defect state density (N_t) with a structure of ITO/NiO_x/PVK/perovskite/MoO₃/Au, as shown in Figure S7. The N_t can be extracted from the defect-state-filled limited region on the curves according to the following equation:

$$N_t = \frac{2V_{TFL}\epsilon\epsilon_0}{eL^2}$$

where ϵ is the relative dielectric constant of perovskite,[54] ϵ_0 is the vacuum permittivity, e is the elementary charge, L is the thickness of the perovskite film, V_{TFL} is the onset voltage of the defect-state-filled limit region. V_{TFL} values extracted by fitting the curves are 0.53 V and 0.34 V for without/with TEOS perovskite films, respectively. The corresponding N_t of the pristine perovskite film is $1.04 \times 10^{17} \text{ cm}^{-3}$. Upon incorporating TEOS, N_t reduces to $6.7 \times 10^{16} \text{ cm}^{-3}$. The reduced N_t indicates the effective passivation effect of the TEOS network.

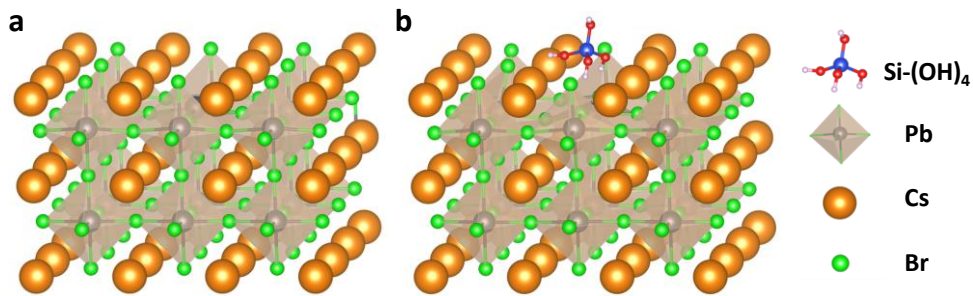


Figure 3. (a) Br defect-containing (100) surface of CsPbBr₃. (b) Adsorption configuration of Si(OH)₄ on the CsPbBr₃ surface with Br defect.

The density functional theory (DFT) calculations are performed to determine the passivation mechanism of TEOS on CsPbBr₃ surface, as shown in Figure 3. The (100) slab of the cubic CsPbBr₃ terminated by Cs and Br atoms was chosen as the surface model. When there is a Br vacancy on the surface, the subsurface Pb atom would become unsaturated, which leads to non-

radiation recombination.[35, 36] According to the DFT calculation, the $\text{Si}(\text{OH})_4$ can effectively fill the Br^- vacancy by decreasing the surface free energy, and thus reduce the non-radiation recombination. The adsorption energy of $\text{Si}(\text{OH})_4$ on the Br vacancy-containing CsPbBr_3 surface is as large as 1.05 eV, which indicates $\text{Si}(\text{OH})_4$ could successfully passivate the defect state and diminish surface recombination.

Figure 4a is the cross-sectional SEM image of devices. NiO_x and the PVK are deposited onto ITO in sequence as the hole injection and transport layer, respectively. The perovskite film that is deposited onto PVK film acting as the emitting layer. TPBi and LiF are thermally evaporated onto the perovskite film as the electron transport and injection layer. As shown in Figure 4b, the band energy level diagram of PeLEDs shows the cascade energy level of NiO_x /PVK, which favors reducing the hole injection barrier.[40] Meanwhile, LiF/TPBi can improve the electron injection from cathode to perovskite. Excitons are formed from the injected holes and electrons due to the quantum confinement of 2D perovskite materials, followed by photon emission through the radiative recombination.

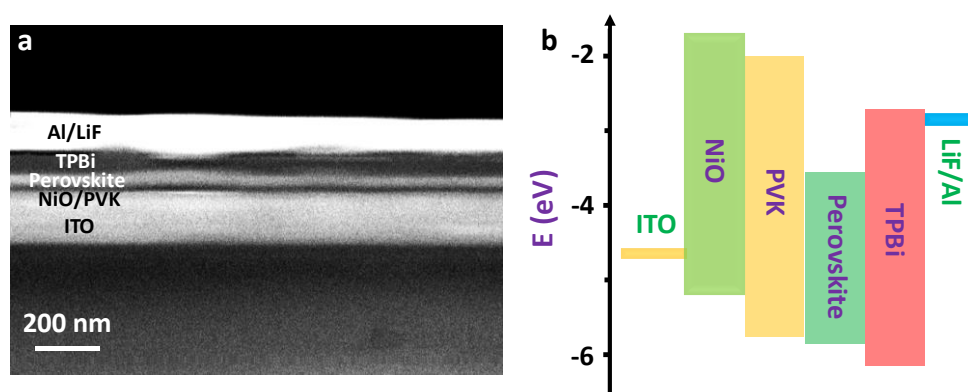


Figure 4. (a) Cross-sectional SEM image and (b) Band energy level diagram of PeLEDs.

Figure 5 and Figure S8 show the electrical characteristics of PeLEDs, and the performances are summarized in Table S1. Figure 5a is the electroluminescence (EL) spectra of a perovskite-TEOS device under different voltage. The EL emission peak of the device is located at 514 nm with a full width at half maximum of 23 nm, which is comparable with the previous PeLED.[29] The EL can keep a stable emission peak at 514 nm with the voltage increase from 4.0 V to 7.0 V. The inset in Figure 5a is a photograph of a demo of a PeLED with an area of $\sim 1 \text{ cm}^2$ under 5 V bias. Furthermore, the corresponding Commission Internationale de l'Eclairage color

coordinate is at (0.12, 0.74) as shown in Figure S9. Meanwhile, the EL emission peak (Figure S10) of the reference device is also located at 514 nm. However, the luminance of the reference device is lower than that of perovskite-TEOS one, as shown in the luminance-voltage curves in Figure 5b. The maximum luminance of perovskite-TEOS device reaches 11330 cd/m^2 at 6.5 V. The maximum luminance of the reference device is 9260 cd/m^2 at 6.5 V. The enhanced luminance upon perovskite-TEOS should be ascribed to the passivation of defect states. Additionally, according to the current density-voltage (J-V) curves in Figure 5b, the device without TEOS demonstrates a poor diode characteristic before the open voltage of 3.0 V, which is due to the leakage current. Upon incorporating TEOS, the leakage current is suppressed to as low as $\sim 10^{-4}$ mA/cm^2 when the voltage is lower than 2.5 V, and consequently, the device shows better diode characteristics. The current efficiency (η_c) and EQE curves are shown in Figure 5c. The reference device presents a η_c of 44.2 cd/A , corresponding to an EQE of 14.0%. However, the η_c improves to 54.4 cd/A in a TEOS based device. And the corresponding EQE reaches 16.6%. Statistical data of devices are summarized in Table S2. Average values of EQE are $16.08 \pm 0.61\%$ and $13.00 \pm 0.53\%$ for devices with and without TEOS, respectively.

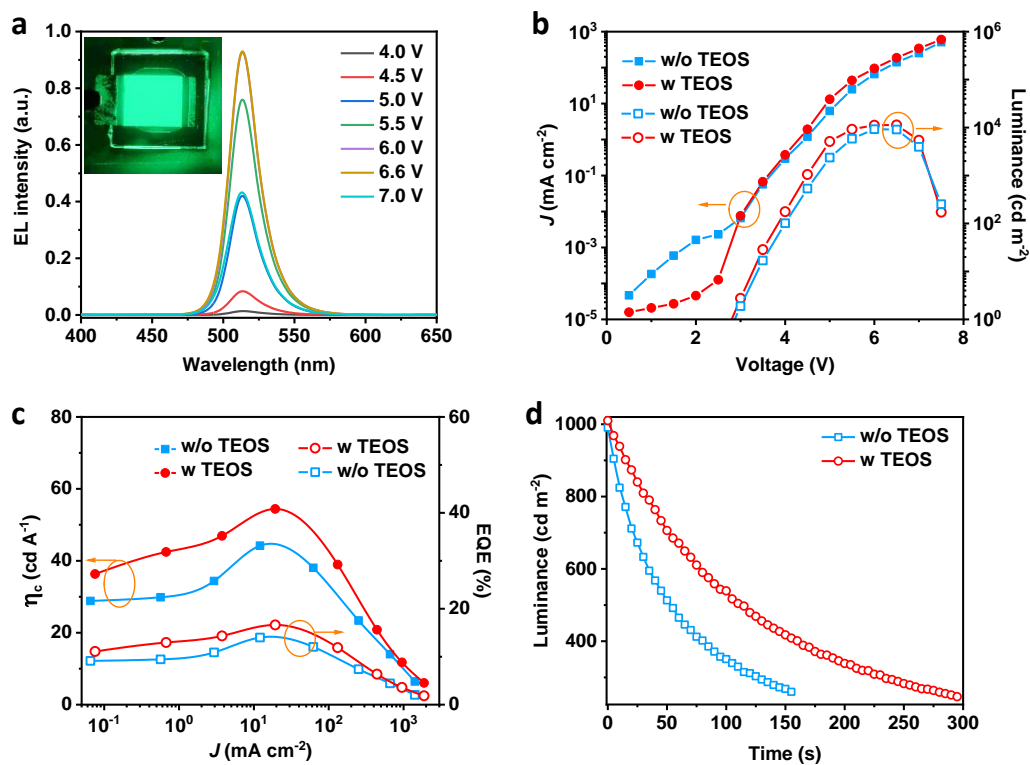


Figure 5. (a) EL spectra of a PeLED with perovskite-TEOS as the emitting layer. The inset shows a photograph of a demo of a ~ 1 cm² device under 5 V bias. (b) J-V and luminance-

voltage curves, (c) η_c and EQE curves, and (d) working stability of devices with and without TEOS network.

The device operational stability was also explored, as shown in Figure 5d of luminance changed with the operation time, where the initial luminance is 1000 cd/m². The half-lifetime of perovskite-TEOS device displays two minutes, which is double of reference one. When the initial luminance is 100 cd/m², the half-lifetime of perovskite-TEOS device reaches 28 minutes, as shown in Figure S11. Joule heat caused by non-radiative recombination is likely a dominating factor resulting in poor working stability.[55] The defect site can trap the injected charges, and then cause the non-radiative recombination of these charges directly. Meanwhile, the excitons formed from the injected charges also have a large quenching probability. The excitons formed in the perovskite film are neutral. The defect states of undercoordinated Pb²⁺ ions in the 2D perovskite are equal to a charged system. These Pb²⁺ ions break the neutral property of excitons, and then cause these excitons quenching instead of radiative recombination.[56] Therefore, defects have to be passivated. In this case, upon charge compensation of the undercoordinated Pb²⁺ ions by the TEOS network, both the non-radiative recombination events and exciton quenching phenomena are suppressed. Consequently, the operational stability of PeLEDs is improved. Additionally, other traditional passivation agents, including 2,2'-(ethylenedioxy)diethylamine (EDEA) with amine group,[24] trioctylphosphine oxide (TOPO) with phosphate group,[31] and poly(ethyleneoxide) (PEO) with ethoxide group,[57] were chosen as alternative additives in PeLEDs to compare the working stability. The half-lifetime of PeLEDs were 42 s, 11 min, 18 min, and 28 min with different additives of EDEA, TOPO, PEO and TEOS, respectively (Figure S11). Because EDEA, TOPO, and PEO would likely be detached/vaporized during the device operation process, the devices with these materials demonstrated relatively poor stability. Crosslinked TEOS could anchor with perovskites owing to the strong interaction between TEOS and perovskites, which resulted in TEOS being more stable during working process, realizing a longer half-lifetime.

Conclusion

In conclusion, we have demonstrated a self-crosslinkable TEOS network in perovskite film to improve the efficiency of PeLEDs. The lone pair electrons from TEOS network coordinate with the undercoordinated Pb^{2+} ions in 2D perovskite through the formation of a Lewis adduct. This interaction passivates the defect state of the perovskite film. The lower concentration of defect states is favorable for reducing non-radiative recombination events. The perovskite-TEOS LED yields an EQE of 16.6% with a luminance of 11330 cd/m^2 . The perovskite-TEOS device achieves two times half-lifetime than the reference one. This work proposed as an alternative path to target high performance perovskite devices *via* an in-situ crosslinked strategy.

Appendix A. Supporting information

Supplementary data associated with this article can be found in the online version.

Acknowledgments

Y. L. and B. S. acknowledge the National Natural Science Foundation of China (91833303, 61974098 and 61674108), the National Key Research and Development Program (2016YFA0201900), Jiangsu High Educational Natural Science Foundation (18KJA430012), the 111 Program and Collaborative Innovation Center of Suzhou Nano Science and Technology, the Priority Academic Program Development of Jiangsu Higher Education Institutions and Collaborative Innovation Center of Suzhou Nano Science & Technology. Y. L., L. K. O. and Y. B. Q. acknowledge the funding support from the Energy Materials and Surface Sciences Unit of the Okinawa Institute of Science and Technology Graduate University, the OIST R&D Cluster Research Program, and the OIST Proof of Concept (POC) Program.

References

- [1] L.N. Quan, B.P. Rand, R.H. Friend, S.G. Mhaisalkar, T.W. Lee, E.H. Sargent, *Chem. Rev.*, 119 (2019) 7444-7477.
- [2] S.D. Stranks, H.J. Snaith, *Nat. Nanotechnol.*, 10 (2015) 391-402.
- [3] Q. Shan, J. Song, Y. Zou, J. Li, L. Xu, J. Xue, Y. Dong, B. Han, J. Chen, H. Zeng, *Small*, 13 (2017) 1701770.

- [4] N.K. Kumawat, X.K. Liu, D. Kabra, F. Gao, *Nanoscale*, 11 (2019) 2109-2120.
- [5] Z.K. Tan, R.S. Moghaddam, M.L. Lai, P. Docampo, R. Higler, F. Deschler, M. Price, A. Sadhanala, L.M. Pazos, D. Credgington, F. Hanusch, T. Bein, H.J. Snaith, R.H. Friend, *Nat. Nanotechnol.*, 9 (2014) 687-692.
- [6] M. Lu, X. Zhang, X. Bai, H. Wu, X. Shen, Y. Zhang, W. Zhang, W. Zheng, H. Song, W.W. Yu, A.L. Rogach, *ACS Energy Lett.*, 3 (2018) 1571-1577.
- [7] S. Zou, Y. Liu, J. Li, C. Liu, R. Feng, F. Jiang, Y. Li, J. Song, H. Zeng, M. Hong, X. Chen, *J. Am. Chem. Soc.*, 139 (2017) 11443-11450.
- [8] G. Pan, X. Bai, W. Xu, X. Chen, D. Zhou, J. Zhu, H. Shao, Y. Zhai, B. Dong, L. Xu, H. Song, *ACS Appl. Mater. Interfaces*, 10 (2018) 39040-39048.
- [9] H. Cho, S.H. Jeong, M.H. Park, Y.H. Kim, C. Wolf, C.L. Lee, J.H. Heo, A. Sadhanala, N. Myoung, S. Yoo, S.H. Im, R.H. Friend, T.W. Lee, *Science*, 350 (2015) 1222-1225.
- [10] S. Kumar, J. Jagielski, S. Yakunin, P. Rice, Y.C. Chiu, M. Wang, G. Nedelcu, Y. Kim, S. Lin, E.J. Santos, M.V. Kovalenko, C.J. Shih, *ACS Nano*, 10 (2016) 9720-9729.
- [11] Z. Chen, Z. Li, C. Zhang, X.F. Jiang, D. Chen, Q. Xue, M. Liu, S. Su, H.L. Yip, Y. Cao, *Adv. Mater.*, 30 (2018) 1801370.
- [12] J. Li, L. Xu, T. Wang, J. Song, J. Chen, J. Xue, Y. Dong, B. Cai, Q. Shan, B. Han, H. Zeng, *Adv. Mater.*, 29 (2017) 1603885.
- [13] J. Song, T. Fang, J. Li, L. Xu, F. Zhang, B. Han, Q. Shan, H. Zeng, *Adv. Mater.*, 30 (2018) 1805409.
- [14] Y. Ling, Z. Yuan, Y. Tian, X. Wang, J.C. Wang, Y. Xin, K. Hanson, B. Ma, H. Gao, *Adv. Mater.*, 28 (2016) 305-311.
- [15] H.C. Wang, W. Wang, A.C. Tang, H.Y. Tsai, Z. Bao, T. Ihara, N. Yarita, H. Tahara, Y. Kanemitsu, S. Chen, R.S. Liu, *Angew. Chem. Int. Ed.*, 56 (2017) 13650-13654.
- [16] X. Shen, Y. Zhang, S.V. Kershaw, T. Li, C. Wang, X. Zhang, W. Wang, D. Li, Y. Wang, M. Lu, L. Zhang, C. Sun, D. Zhao, G. Qin, X. Bai, W.W. Yu, A.L. Rogach, *Nano Lett.*, 19 (2019) 1552-1559.
- [17] J.W. Lee, Y.J. Choi, J.M. Yang, S. Ham, S.K. Jeon, J.Y. Lee, Y.H. Song, E.K. Ji, D.H. Yoon, S. Seo, H. Shin, G.S. Han, H.S. Jung, D. Kim, N.G. Park, *ACS Nano*, 11 (2017) 3311-3319.
- [18] L. Zhao, Y.W. Yeh, N.L. Tran, F. Wu, Z. Xiao, R.A. Kerner, Y.L. Lin, G.D. Scholes, N.

- Yao, B.P. Rand, *ACS Nano*, 11 (2017) 3957-3964.
- [19] S. Lee, C.H. Jang, T.L. Nguyen, S.H. Kim, K.M. Lee, K. Chang, S.S. Choi, S.K. Kwak, H.Y. Woo, M.H. Song, *Adv. Mater.*, 31 (2019) 1900067.
- [20] Y. Liu, J.Y. Cui, K. Du, H. Tian, Z.F. He, Q.H. Zhou, Z.L. Yang, Y.Z. Deng, D. Chen, X.B. Zuo, Y. Ren, L. Wang, H.M. Zhu, B.D. Zhao, D.W. Di, J.P. Wang, R.H. Friend, Y.Z. Jin, *Nat. Photonics*, 13 (2019) 760-764.
- [21] K. Lin, J. Xing, L.N. Quan, F.P.G. de Arquer, X. Gong, J. Lu, L. Xie, W. Zhao, D. Zhang, C. Yan, W. Li, X. Liu, Y. Lu, J. Kirman, E.H. Sargent, Q. Xiong, Z. Wei, *Nature*, 562 (2018) 245-248.
- [22] T. Chiba, Y. Hayashi, H. Ebe, K. Hoshi, J. Sato, S. Sato, Y.J. Pu, S. Ohisa, J. Kido, *Nat. Photonics*, 12 (2018) 681-687.
- [23] X. Zhao, Z.-K. Tan, *Nat. Photonics*, 14 (2019) 215-218.
- [24] W.D. Xu, Q. Hu, S. Bai, C.X. Bao, Y.F. Miao, Z.C. Yuan, T. Borzda, A.J. Barker, E. Tyukalova, Z.J. Hu, M. Kawecki, H.Y. Wang, Z.B. Yan, X.J. Liu, X.B. Shi, K. Uvdal, M. Fahlman, W.J. Zhang, M. Duchamp, J.M. Liu, A. Petrozza, J.P. Wang, L.M. Liu, W. Huang, F. Gao, *Nat. Photonics*, 13 (2019) 418-424.
- [25] L.N. Quan, F.P. Garcia de Arquer, R.P. Sabatini, E.H. Sargent, *Adv. Mater.*, 30 (2018) 1801996.
- [26] S. Chen, G. Shi, *Adv. Mater.*, 29 (2017) 1605448.
- [27] M. Yuan, L.N. Quan, R. Comin, G. Walters, R. Sabatini, O. Voznyy, S. Hoogland, Y. Zhao, E.M. Beauregard, P. Kanjanaboos, Z. Lu, D.H. Kim, E.H. Sargent, *Nat. Nanotechnol.*, 11 (2016) 872-877.
- [28] N. Wang, L. Cheng, R. Ge, S. Zhang, Y. Miao, W. Zou, C. Yi, Y. Sun, Y. Cao, R. Yang, Y. Wei, Q. Guo, Y. Ke, M. Yu, Y. Jin, Y. Liu, Q. Ding, D. Di, L. Yang, G. Xing, H. Tian, C. Jin, F. Gao, R.H. Friend, J. Wang, W. Huang, *Nat. Photonics*, 10 (2016) 699-704.
- [29] M. Ban, Y. Zou, J.P.H. Rivett, Y. Yang, T.H. Thomas, Y. Tan, T. Song, X. Gao, D. Credington, F. Deschler, H. Siringhaus, B. Sun, *Nat. Commun.*, 9 (2018) 3892.
- [30] B.D. Zhao, S. Bai, V. Kim, R. Lamboll, R. Shivanna, F. Auras, J.M. Richter, L. Yang, L.J. Dai, M. Alsari, X.J. She, L.S. Liang, J.B. Zhang, S. Lilliu, P. Gao, H.J. Snaith, J.P. Wang, N.C. Greenham, R.H. Friend, D.W. Di, *Nat. Photonics*, 12 (2018) 783-789.

- [31] X. Yang, X. Zhang, J. Deng, Z. Chu, Q. Jiang, J. Meng, P. Wang, L. Zhang, Z. Yin, J. You, *Nat. Commun.*, 9 (2018) 570.
- [32] S. Lee, D.B. Kim, J.C. Yu, C.H. Jang, J.H. Park, B.R. Lee, M.H. Song, *Adv. Mater.*, 31 (2019) 1805244.
- [33] J.W. Lee, H.S. Kim, N.G. Park, *Acc Chem Res*, 49 (2016) 311-319.
- [34] D.P. Nenon, K. Pressler, J. Kang, B.A. Koscher, J.H. Olshansky, W.T. Osowiecki, M.A. Koc, L.W. Wang, A.P. Alivisatos, *J. Am. Chem. Soc.*, 140 (2018) 17760-17772.
- [35] B. Chen, P.N. Rudd, S. Yang, Y. Yuan, J. Huang, *Chem. Soc. Rev.*, 48 (2019) 3842-3867.
- [36] L.K. Ono, S.F. Liu, Y.B. Qi, *Angew. Chem. Int. Ed.*, 59 (2020) 2-25.
- [37] G. Li, F.W. Rivarola, N.J. Davis, S. Bai, T.C. Jellicoe, F. de la Pena, S. Hou, C. Ducati, F. Gao, R.H. Friend, N.C. Greenham, Z.K. Tan, *Adv. Mater.*, 28 (2016) 3528-3534.
- [38] L. Song, X. Guo, Y. Hu, Y. Lv, J. Lin, Z. Liu, Y. Fan, X. Liu, *J. Phys. Chem. Lett.*, 8 (2017) 4148-4154.
- [39] L.-P. Cheng, J.-S. Huang, Y. Shen, G.-P. Li, X.-K. Liu, W. Li, Y.-H. Wang, Y.-Q. Li, Y. Jiang, F. Gao, C.-S. Lee, J.-X. Tang, *Adv. Opt. Mater.*, 7 (2018) 1801534.
- [40] Y. Liu, T. Wu, Y. Liu, T. Song, B. Sun, *APL Mater.*, 7 (2019) 021102.
- [41] G. Kresse, J. Furthmüller, *Comput. Mater. Sci.*, 6 (1996) 15-50.
- [42] G. Kresse, J. Furthmüller, *Phys. Rev. B*, 54 (1996) 11169-11186.
- [43] J.P. Perdew, M. Ernzerhof, K. Burke, *J. Chem. Phys.*, 105 (1996) 9982-9985.
- [44] J.P. Perdew, K. Burke, M. Ernzerhof, *Phys. Rev. Lett.*, 77 (1996) 3865-3868.
- [45] P.E. Blöchl, *Phys. Rev. B*, 50 (1994) 17953-17979.
- [46] S. Grimme, J. Antony, S. Ehrlich, H. Krieg, *J. Chem. Phys.*, 132 (2010) 154104.
- [47] R. Al-Oweini, H. El-Rassy, *J. Mol. Struct.*, 919 (2009) 140-145.
- [48] R. Wang, J. Xue, L. Meng, J.-W. Lee, Z. Zhao, P. Sun, L. Cai, T. Huang, Z. Wang, Z.-K. Wang, Y. Duan, J.L. Yang, S. Tan, Y. Yuan, Y. Huang, Y. Yang, *Joule*, 3 (2019) 1464-1477.
- [49] L. Xie, J. Chen, P. Vashishtha, X. Zhao, G.S. Shin, S.G. Mhaisalkar, N.-G. Park, *ACS Energy Lett.*, 4 (2019) 2192-2200.
- [50] Y. Tian, C. Zhou, M. Worku, X. Wang, Y. Ling, H. Gao, Y. Zhou, Y. Miao, J. Guan, B. Ma, *Adv. Mater.*, 30 (2018) 1707093.
- [51] Z. Xiao, R.A. Kerner, L. Zhao, N.L. Tran, K.M. Lee, T.-W. Koh, G.D. Scholes, B.P. Rand,

Nat. Photonics, 11 (2017) 108-115.

[52] Z.G. Xiao, R.A. Kerner, N. Tran, L.F. Zhao, G.D. Scholes, B.P. Rand, *Adv. Funct. Mater.*, 29 (2019) 1807284.

[53] Z.F. Wu, M.W. Jiang, Z.H. Liu, A. Jamshaid, L.K. Ono, Y.B. Qi, *Adv. Energy Mater.*, 10 (2020) 1903696.

[54] D. Saponi, M. Kepenekian, L. Pedesseau, C. Katan, J. Even, *Nanoscale*, 8 (2016) 6369-6378.

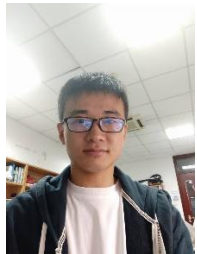
[55] H. Kim, L. Zhao, J.S. Price, A.J. Grede, K. Roh, A.N. Brigeman, M. Lopez, B.P. Rand, N.C. Giebink, *Nat. Commun.*, 9 (2018) 4893.

[56] C. Javaux, B. Mahler, B. Dubertret, A. Shabaev, A.V. Rodina, A.L. Efros, D.R. Yakovlev, F. Liu, M. Bayer, G. Camps, L. Biadala, S. Buil, X. Quelin, J.P. Hermier, *Nat. Nanotechnol.*, 8 (2013) 206-212.

[57]] J. Li, S.G. Bade, X. Shan, Z. Yu, *Adv. Mater.*, 27 (2015) 5196-5202.



Yuqiang Liu is a postdoctoral scholar in Energy Materials and Surface Sciences Unit at Okinawa Institute of Science and Technology Graduate University in Japan. He obtained his Ph.D. from Institute of Functional Nano & Soft Materials, Soochow University, China. His current research focuses on recombination mechanism and surface science of perovskite light-emitting diodes.



Lei Cai is a Ph.D. candidate at Institute of Functional Nano & Soft Materials, Soochow University, China. He received his M.S. degree from Shandong Normal University in 2016. His current research focuses on efficient and stable green and blue perovskite light-emitting diodes.



Yafeng Xu received her bachelor degree in Materials Science and Engineering from Henan Polytechnic University in 2017 and now is a master student at the Institute of Functional Nano & Soft Materials of Soochow University. Her current research mainly focuses on the simulation and design of functional nanomaterials based first-principles calculations.



Junnan Li is a postgraduate candidate in Institute of Functional Nano & Soft Materials,

Soochow University, China. His current research field focuses on defects passivation and device engineering of perovskite light-emitting diodes.



Yuanshuai Qin is a postgraduate candidate in Institute of Functional Nano & Soft Materials, Soochow University, China. His current research interests focus on fabrication and application of silicon nanostructure and advanced energy-related devices.



Tao Song is an Associate Professor in Institute of Functional Nano & Soft Materials, Soochow University, China. He received his Ph.D. in physics from Soochow University, China. His main research fields are hybrid solar cells based on conjugated polymer/inorganic nanostructures and efficient perovskite/quantum dots light emitting diodes.



Lu Wang is an Associate Professor in Institute of Functional Nano & Soft Materials, Soochow University, China. She received her Ph.D. in Chemistry Materials at Dalian University of Technology in 2011. After being a postdoctoral in The Hong Kong Polytechnic University (2011-2013), she joined Institute of Functional and Soft Materials in 2013. Her main research field is energy calculations for complicated nanostructured materials.



Youyong Li is a Professor in Institute of Functional Nano & Soft Materials, Soochow University, China. He received his Ph.D. in Chemistry, California Institute of Technology in 2004. After being a postdoctoral (2004-2005) and Director of functional material and biotech (2006-2009) in California Institute of Technology. He joined Institute of Functional and Soft Materials in 2009. His main research field is methodologies for free energy calculations and Monte Carlo methods to study complicated molecules and materials.



Luis K. Ono is a staff scientist in Prof. Yabing Qi's Research Unit (Energy Materials and Surface Sciences Unit) at Okinawa Institute of Science and Technology Graduate University in Japan. He obtained his B.S. in Physics/Microelectronics from the University of São Paulo, Brazil. Later he joined the Department of Nuclear Engineering in Kyoto University, Japan, and the University of Central Florida, USA, where he obtained his M.S. and Ph.D., respectively. His current research focuses on the fundamental understanding and surface science aspects of perovskite solar cells.



Yabing Qi is Professor and Unit Director of Energy Materials and Surface Sciences Unit (EMSSU) at Okinawa Institute of Science and Technology Graduate University (OIST) in Japan, and a Fellow of the Royal Society of Chemistry (FRSC). Before joining OIST, Prof. Qi was a postdoctoral fellow at Princeton University. Prof. Qi received his B.S., M.Phil., and Ph.D. from Nanjing University, Hong Kong University of Science and Technology, and University of California Berkeley, respectively. His research interests include surface / interface sciences, perovskite solar cells, lithium ion batteries, organic electronics, energy materials and devices (<https://groups.oist.jp/emssu>).



Baoquan Sun is a Professor in Institute of Functional Nano & Soft Materials, Soochow University, China. He received his Ph.D. in Chemistry Materials at Tsinghua University in Beijing in 2002. After being a postdoctoral in Cavendish Laboratory at Cambridge University (2002-2007) and Los Alamos National Laboratory (2007-2008), he joined Institute of Functional and Soft Materials in 2008. His main research fields are nanostructured semiconductor materials, conducting ink, charge separation and transport, interface engineering for flexible electronics, light emitting diodes and organic/inorganic heterojunction solar cells.